# Inorganic Chemistry

**Article**

# Valence-State Alternatives in Diastereoisomeric Complexes [(acac)$_2$Ru($\mu$-QL)Ru(acac)$_2$]$^n$ (QL$^{2-}$ = 1,4-Dioxido-9,10-anthraquinone, $n$ = +2, +1, 0, −1, −2)

**Somnath Maji,[†] Biprajit Sarkar,[‡] Shaikh M. Mobin,[†] Jan Fiedler,[§] Francisco A. Urbanos,[‖]**
**Reyes Jimenez-Aparicio,*,[‖] Wolfgang Kaim,*,[‡] and Goutam Kumar Lahiri*,[†]**

*Department of Chemistry, Indian Institute of Technology, Bombay, Powai, Mumbai-400076, India,*
*Institut für Anorganische Chemie, Universität Stuttgart, Pfaffenwaldring 55, D-70550 Stuttgart,*
*Germany, J. Heyrovský Institute of Physical Chemistry, v.v.i., Academy of Sciences of the Czech*
*Republic, Dolejškova 3, CZ-18223 Prague, Czech Republic, Departamento de Quimica Inorganica,*
*Facultad de Ciencias Quimicas, Universidad Complutenses, Ciudad Universitaria,*
*E-28040 Madrid, Spain*

The title complexes were obtained in neutral form ($n$ = 0) as *rac* (**1**) and *meso* isomers (**2**). **2** was crystallized for X-ray diffraction and its temperature-dependent magnetism studied. It contains two antiferromagnetically coupled ruthenium(III) ions, bridged by the quinizarine dianion QL$^{2-}$ (quinizarine = 1,4-dihydroxy-9,10-anthraquinone). The potential of both the ligand (QL$^{0}$ → QL$^{4-}$) and the metal complex fragment combination [(acac)$_2$Ru$^{II}$]$_2$ → {[(acac)$_2$Ru$^{IV}$]$_2$}$^{4+}$ to exist in five different redox states creates a large variety of combinations, which was assessed for the electrochemically reversibly accessible 2+, 1+, 0, 1−, 2− forms using cyclic voltammetry as well as EPR and UV-vis-NIR spectroelectrochemistry. The results for the two isomers are similar: Oxidation to **1**$^+$ or **2**$^+$ causes the emergence of a near-infrared band (1390 nm), without revealing an EPR response even at 4 K. Reduction to **1**$^-$ or **2**$^-$ produces an EPR signal, signifying metal-centered spin but no near-infrared absorption. Tentatively, we assume metal-based oxidation of [(acac)$_2$Ru$^{III}$($\mu$-QL$^{2-}$)Ru$^{III}$(acac)$_2$] to a mixed-valent intermediate [(acac)$_2$Ru$^{III}$($\mu$-QL$^{2-}$)Ru$^{IV}$(acac)$_2$]$^+$ and ligand-centered reduction to a radical complex [(acac)$_2$Ru$^{III}$($\mu$-QL$^{\cdot 3-}$)Ru$^{III}$(acac)$_2$]$^-$ with antiferromagnetic three-spin interaction.

## Introduction

The establishment of delicate metal−ligand valence state balance in various redox forms of ruthenium−quinone frameworks has turned out to be a formidable challenge due to the remarkable mixing of the frontier orbitals of ruthenium and of quinonoid ligands.[1] Moreover, the electronic features of the ancillary ligands (AL) in such complexes contribute significantly to the valence-state combination. Therefore, a variety of mononuclear[2] and a few polynuclear ruthenium−

quinonoid[3] systems have been scrutinized over the years in combination with different coligands. In a different context, 1,4-dihydroxy-9,10-anthraquinone (quinizarine, QLH$_2$), a biologically relevant molecule,[4] has been used in a variety of mononuclear,[5] dinuclear[6] and coordination polymeric[7] metal complexes. However, only two diruthenium derivatives of QL$^{2-}$, [{(AL)$_2$Ru$^{II}$}$_2$(QL$^{2-}$)]$^{2+}$ where AL = pap = 2-phenylazopyridine[6a] and AL = bpy = 2,2'-bipyridine[6b,c] have been reported. The latter were studied with respect to mixed valency[6b] and optical nonlinearity.[6c] The present article originates from perspectives of establishing the valence-state distribution in {(acac)$_2$Ru($\mu$-QL$^{2-}$)Ru(acac)$_2$}$^n$ (acac$^-$ = acetylacetonato = 2,4-pentanedionato), including the exploration of mixed-valent intermediates. The choice of acac$^-$ as ancillary ligands has been prompted by our observation that the association of $\sigma$-donating acac$^-$ with ruthenium can introduce substantial variations in (i) the metal−ligand

* To whom correspondence should be addressed. E-mail: kaim@iac.uni-stuttgart.de (W.K.), lahiri@chem.iitb.ac.in (G.K.L.).
† Indian Institute of Technology.
‡ Universität Stuttgart.
§ Academy of Sciences of the Czech Republic.
‖ Universidad Complutense.
(1) (a) DelMedico, A.; Dodsworth, E. S.; Lever, A. B. P.; Pietro, W. J. *Inorg. Chem.* **2004**, *43*, 2654. (b) da Cunha, C. J.; Dodsworth, E. S.; Monteiro, M. A.; Lever, A. B. P. *Inorg. Chem.* **1999**, *38*, 5399.

valence combinations,[2a,3a,b,8] (ii) the intermetallic electronic coupling in mixed-valent diruthenium and triruthenium systems,[9] and (iii) the intramolecular chemical transformation potential.[10]

Herein, we report the one-pot synthesis of diastereomeric[11] complexes $[(acac)_2Ru^{III}(\mu\text{-}QL^{2-})Ru^{III}(acac)_2]^n$ ($n = 0$; $\Delta\Delta/\Lambda\Lambda$, *rac*, **1** and $\Delta\Lambda$, *meso*, **2**), the magnetic properties, and the crystal structure of **2**. The metal−ligand valence-state distribution in $\mathbf{1}^n$ and $\mathbf{2}^n$, $n = -2, -1, 0, +1, +2$ has been assessed via UV-vis-NIR spectroelectrochemistry and EPR investigations.

## Results and Discussion

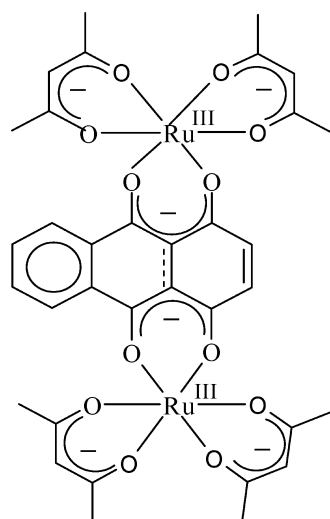**Synthesis and Characterization of 1 and 2.** The mixture of diastereomeric complexes $[(acac)_2Ru^{III}(\mu\text{-}QL^{2-})Ru^{III}(acac)_2]$, **1**: $\Delta\Delta/\Lambda\Lambda$, *rac* and **2**: $\Delta\Lambda$, *meso*) has been obtained via the reaction of quinizarine, QLH$_2$, with the precursor $Ru(acac)_2(CH_3CN)_2$ in the presence of NaOAc under aerobic conditions, followed by chromatographic purification using silica gel. Diastereomers **1** and **2** have been separated on a preparatory silica gel TLC plate (Scheme 1). In addition to NMR spectroscopy, the meso isomer (**2**) has been authenticated by its single crystal X-ray structure (later).

The positive ion electrospray mass spectra of the diastereomers (Supporting Information, Figure S1) agree with the formulation as do the microanalytical data (Experimental Section). The effect of anionic ancillary and bridging ligands in the complexes is reflected by the stabilization of the $Ru^{III}$−$Ru^{III}$ configuration obtained from ruthenium(II) precursors under aerobic experimental conditions. At 300 K, under a magnetic field of 10 000 G, **1** and **2** exhibit magnetic moments of 2.59 and 2.23 $\mu_B$, respectively, indicating that the ruthenium(III) centers are weakly antiferromagnetically coupled (later).

The molecular structure of **2** is shown in Figure 1. Selected crystallographic parameters and bond distances/angles are

(2) (a) Patra, S.; Sarkar, B.; Mobin, S. M.; Kaim, W.; Lahiri, G. K. *Inorg. Chem.* **2003**, *43*, 6469. (b) Maji, S.; Patra, S.; Chakraborty, S.; Mobin, S. M.; Janardanan, D.; Sunoj, R. B.; Lahiri, G. K. *Eur. J. Inorg. Chem.* **2007**, 314. (c) Bag, N.; Lahiri, G. K.; Basu, P.; Chakravorty, A. *J. Chem. Soc., Dalton Trans.* **1992**, 113. (d) Bag, N.; Pramanik, A.; Lahiri, G. K.; Chakravorty, A. *Inorg. Chem.* **1992**, *31*, 40. (e) Remenyi, C.; Kaupp, M. *J. Am. Chem. Soc.* **2005**, *127*, 11399. (f) Ebadi, M.; Lever, A. B. P. *Inorg. Chem.* **1999**, *38*, 467. (g) Metcalfe, R. A.; Lever, A. B. P. *Inorg. Chem.* **1997**, *36*, 4762. (h) Masui, H.; Lever, A. B. P.; Dodsworth, E. S. *Inorg. Chem.* **1993**, *32*, 258. (i) Schwederski, B.; Kaim, W. *Inorg. Chim. Acta* **1992**, *195*, 123. (j) Masui, H.; Lever, A. B. P.; Auburn, P. *Inorg. Chem.* **1991**, *30*, 2402. (k) Haga, M.; Dodsworth, E. S.; Lever, A. B. P. *Inorg. Chem.* **1986**, *25*, 447. (l) Salmonsen, R. B.; Abelleira, A.; Clarke, M. J. *Inorg. Chem.* **1984**, *23*, 385. (m) Waldhör, E.; Schwederski, B.; Kaim, W. *J. Chem. Soc., Perkin Trans.* **1993**, 2109. (n) Pierpont, C. G. *Coord. Chem. Rev.* **2001**, *219−221*, 415. (o) Pierpont, C. G.; Attia, A. S. *Collect. Czech. Chem. Commun.* **2001**, *66*, 33. (p) Pierpont, C. G.; Lange, C. W. *Prog. Inorg. Chem.* **1994**, *41*, 331. (q) Dei, A.; Gatteschi, D.; Sangregorio, C.; Sorace, L. *Acc. Chem. Res.* **2004**, *37*, 827. (r) Lever, A. B. P.; Gorelsky, S. I. *Coord. Chem. Rev.* **2000**, *208*, 153. (s) Bhattacharya, S. *Polyhedron* **1994**, *13*, 451. (t) Kurihara, M.; Daniele, S.; Tsuge, K.; Sugimoto, H.; Tanaka, K. *Bull. Chem. Soc. Jpn.* **1998**, *71*, 867. (u) Gorelsky, S. I.; Lever, A. B. P.; Ebadi, M. *Coord. Chem. Rev.* **2002**, *230*, 97.

(3) (a) Kar, S.; Sarkar, B.; Ghumaan, S.; Janardanan, D.; van Slageren, J.; Fiedlar, J.; Puranik, V. G.; Sunoj, R, V.; Kaim, W.; Lahiri, G. K. *Chem.−Eur. J.* **2005**, *11*, 4901. (b) Patra, S.; Sarkar, B.; Ghumaan, S.; Fiedler, J.; Zalis, S.; Kaim, W.; Lahiri, G. K. *Dalton Trans.* **2004**, 750. (c) Chakarborty, S.; Laye, R. H.; Paul, R. L.; Gonnade, R. G.; Puranik, V. G.; Ward, M. D.; Lahiri, G. K. *J. Chem. Soc., Dalton Trans.* **2002**, 1172. (d) Ghumaan, S.; Sarkar, B.; Patra, S.; van Slageren, J.; Fiedler, J.; Kaim, W.; Lahiri, G. K. *Inorg. Chem.* **2005**, *45*, 3210. (e) Braunstein, P.; Demessence, A.; Siri, O.; Taquet, J.-P. *C. R. Chimie* **2004**, *7*, 909. (f) Masui, H.; Freda, A. L.; Zerner, M. C.; Lever, A. B. P. *Inorg. Chem.* **2000**, *39*, 141. (g) Ernst, S.; Hänel, P.; Jordanov, J.; Kaim, W.; Kasack, V.; Roth, E. *J. Am. Chem. Soc.* **1989**, *111*, 1733. (h) Ernst, S.; Kasack, V.; Bessenbacher, C.; Kaim, W. *Z. Naturforsch.* **1987**, *42b*, 425. (i) Ward, M. D.; McCleverty, J. A. *J. Chem. Soc., Dalton Trans.* **2002**, 275. (j) Kasack, V.; Kaim, W.; Binder, H.; Jordanov, J.; Roth, E. *Inorg. Chem.* **1995**, *34*, 1924. (k) Auburn, P. R.; Lever, A. B. P. *Inorg. Chem.* **1990**, *29*, 2551. (l) Metcalfe, R. A.; Vasconcellos, L. C. G.; Mirza, H.; Franco, D. W.; Lever, A. B. P. *J. Chem. Soc., Dalton Trans.* **1999**, 2653. (m) Shukla, A.; Das, A. *Polyhedron* **2000**, *19*, 2605. (n) Ward, M. D. *Inorg. Chem.* **1996**, *35*, 1712. (o) Dei, A.; Gatteschi, D.; Pardi, L. *Inorg. Chem.* **1990**, *29*, 1442. (p) Bruni, S.; Cariati, F.; Dei, A.; Gatteschi, D. *Inorg. Chim. Acta* **1991**, *186*, 157. (q) Joulie, L. F.; Schatz, E.; Ward, M. D.; Weber, F.; Yellowless, L. J. *J. Chem. Soc., Dalton Trans.* **1994**, 799. (r) Joss, S.; Reust, H.; Ludi, A. *J. Am. Chem. Soc.* **1981**, *103*, 981.

(4) (a) Myers, C.; Gianni, L.; Zweier, J.; Muindi, J.; Sinha, B. K.; Eliot, H. *Fed. Proc., Fed. Am. Soc. Exp. Biol.* **1986**, *45*, 2792. (b) Arcamone, F. *Med. Res. Rev.* **1984**, *4*, 153. (c) Naff, M. B.; Plowman, J.; Narayanan, V. L. In *Anthracycline Antibiotics*; El Khadem, H. S. Ed.; Academic Press: New York, 1982; p 1. (d) Young, R. C.; Ozols, R. F.; Myers, C. E. *Clin. Rev.* **1981**, *305*, 139.

(5) (a) Vaira, M. D.; Orioli, P.; Piccioli, F.; Bruni, B.; Messori, L. *Inorg. Chem.* **2003**, *42*, 3157. (b) Quinti, L.; Allen, N. S.; Edge, M.; Murphy, B. P.; Perotti, A. *J. Photochem. Photobiol., A* **2003**, *155*, 79. (c) Churchill, M. R.; Keil, K. M.; Bright, F. V.; Pandey, S.; Baker, G. A.; Keister, J. B. *Inorg. Chem.* **2000**, *39*, 5807. (d) Churchill, M. R.; Keil, K. M.; Gilmartin, B. P.; Schuster, J. J.; Keister, J. B.; Janik, T. S. *Inorg. Chem.* **2001**, *40*, 4361. (e) Gooden, V. M.; Cai, H.; Dasgupta, T. P.; Gordon, N. R.; Hughes, L. J.; Sadler, G. G. *Inorg. Chim. Acta* **1997**, *255*, 105. (f) Kühlwein, F.; Polborn, K.; Beck, W. Z. *Anorg. Allg. Chem.* **1997**, *623*, 1931. (g) Bodini, M. E.; Arancibia, V. *Polyhedron* **1991**, *10*, 1929. (h) Bottei, R. S.; Lusardi, D. A. *Thermochim. Acta* **1981**, *43*, 355.

(6) (a) Ghumaan, S.; Mukherjee, S.; Kar, S.; Roy, D.; Mobin, S. M.; Sunoj, R. B.; Lahiri, G. K. *Eur. J. Inorg. Chem.* **2006**, *4426*. (b) Sadler, G. G.; Gordon, N. *R. Inorg. Chim. Acta* **1991**, *180*, 271. (c) Sun, W.; Patton, T. H.; Stultz, L. K.; Claude, J. P. *Opt. Commun.* **2003**, *218*, 189. (d) Bodini, M. E.; del Valle, M. A.; Cáceres, S. *Polyhedron* **1997**, *17*, 2903. (e) Bakola-Christianopoulou, M. N.; Akrivos, P. D.; Baumgarten, M. *Can. J. Chem.* **1987**, *65*, 1485. (f) Heinze, K.; Mann, S.; Huttner, G.; Zsolnai, L. *Chem. Ber* **1996**, *129*, 1115. (g) Leschke; M.; Melter, M.; Lang, H. *Inorg. Chim. Acta* **2003**, *350*, 114. (h) Pierpont, C. G.; Francesconi, L. C.; Hendrickson, D. N. *Inorg. Chem.* **1978**, *17*, 3470. (i) Maroney, M. J.; Day, R. O.; Psyris, T.; Fleury, L. M.; Whitehead., J, P. *Inorg. Chem.* **1989**, *28*, 175. (j) Merrell, P. H. *Inorg. Chim. Acta* **1979**, *32*, 99. (k) Venkatesan, R.; Rajendiran, T. M.; Rao, P. S. *Indian J. Chem.* **1998**, *37A*, 280.

(7) (a) Sharma, J.; Singh, H. B. *Inorg. Chim. Acta* **1987**, *133*, 161. (b) Sharma, J.; Singh, H. B.; Rao, T. S. *Curr. Sci.* **1986**, *55*, 345. (c) Singh, H. B.; Sharma, J. *Indian J. Chem.* **1987**, *26A*, 167. (d) Sharma, J.; Singh, H. B.; Rao, T. S. *Indian J. Chem.* **1986**, *25A*, 330.

(8) (a) Patra, S.; Sarkar, B.; Maji, S.; Fiedler, J.; Urbanos, F. A.; Jimenez-Aparicio, R.; Kaim, W.; Lahiri, G. K. *Chem.−Eur. J.* **2005**, *11*, 489. (b) Kar, S.; Sarkar, B.; Ghumaan, S.; Roy, D.; Urbanos, F. A.; Fiedler, J.; Sunoj, R. B.; Jimenez-Aparicio, R.; Kaim, W.; Lahiri, G. K. *Inorg. Chem.* **2005**, *44*, 8715. (c) Sarkar; B.; Patra, S.; Fiedler, J.; Sunoj, R. B.; Janardanan, D.; Mobin, S. M.; Niemeyer, M.; Lahiri, G. K.; Kaim., W. *Angew. Chem., Int. Ed.* **2005**, *44*, 5655.

(9) (a) Patra, S.; Sarkar, B.; Ghumaan, S.; Fiedler, J.; Kaim, W.; Lahiri, G. K. *Inorg. Chem.* **2004**, *43*, 6108. (b) Patra, S.; Sarkar, B.; Ghumaan, S.; Fiedler, J.; Kaim, W.; Lahiri, G. K. *Dalton Trans.* **2004**, *754*. (c) Kar, S.; Chanda, N.; Mobin, S. M.; Datta, A.; Urbanos, F. A.; Puranik, V. G.; Jimenez-Aparicio, R.; Lahiri, G. K. *Inorg. Chem.* **2004**, *43*, 4911. (d) Ghumaan, S.; Sarkar, B.; Patra, S.; Parimal, K.; Slageren, J. V.; Fiedler, J.; Kaim, W.; Lahiri, G. K. *Dalton Trans.* **2005**, 706.

(10) (a) Patra, S.; Miller, T. A.; Sarkar, B.; Niemeyer, M.; Ward, M. D.; Lahiri., G. K. *Inorg. Chem.* **2003**, *42*, 4707. (b) Patra, S.; Mondal, B.; Sarkar, B.; Niemeyer, M.; Lahiri, G. K. *Inorg. Chem.* **2003**, *42*, 1322. (c) Kar, S.; Chanda, N.; Mobin, S. M.; Urbanos, F. A.; Niemeyer, M.; Puranik, V. G.; Jimenez-Aparicio, R.; Lahiri, G. K. *Inorg. Chem.* **2005**, *44*, 1571. (d) Maji, S.; Sarkar, B.; Patra, S.; Fiedler, J.; Mobin, S. M.; Puranik, V. G.; Kaim, W.; Lahiri, G. K. *Inorg. Chem.* **2006**, *45*, 1316.

(11) (a) Keene, F. R. *Chem. Soc. Rev.* **1998**, *27*, 185. (b) D'Alessandro, D. M.; Keene, F. R. *Chem. Phys.* **2006**, *324*, 8.

**Scheme 1**



**1 :** ΔΔ/ΛΛ  (*rac*)
**2 :**   ΔΛ   (*meso*)

**Table 1.** Crystallographic Data for **2**·(C₇H₈)

| mol formula | $C_{41}H_{42}O_{12}Ru_2$ |
|---|---|
| fw | 928.89 |
| cryst syst | triclinic |
| space group | $P\bar{1}$ |
| $a$ (Å) | 12.3262 (18) |
| $b$ (Å) | 12.326 (3) |
| $c$ (Å) | 13.9882 (16) |
| $\alpha$ (deg) | 98.702 (13) |
| $\beta$ (deg) | 105.311 (11) |
| $\gamma$ (deg) | 95.727 (14) |
| $V$ (Å³) | 2004.4 (6) |
| Z | 2 |
| $\mu$ (mm⁻¹) | 0.815 |
| $T$ (K) | 293 (2) |
| $D_{calcd}$ (g cm⁻³) | 1.539 |
| F (000) | 944 |
| $2\theta$ range (deg) | 3.08−49.96 |
| $e$ data ($R_{int}$) | 6996/0.0327 |
| R1, wR2 [$I > 2\sigma(I)$] | 0.0481, 0.1085 |
| R1, wR2(all data) | 0.1292, 0.1307 |
| GOF | 1.013 |
| largest diff. peak/hole, (e Å⁻³) | 0.823 /−0.570 |

**Table 2.** Important Bond Distances (Angstroms) and Angles (Degrees) for **2**·(C₇H₈)

| bond distances | | bond angles | |
|---|---|---|---|
| Ru(1)−O(1) | 2.014(4) | O(1)−Ru(1)−O(5) | 89.05(17) |
| Ru(1)−O(2) | 2.014(4) | O(1)−Ru(1)−O(6) | 90.58(17) |
| Ru(1)−O(3) | 2.015(4) | O(2)−Ru(1)−O(5) | 178.51(17) |
| Ru(1)−O(4) | 1.996(4) | O(2)−Ru(1)−O(6) | 91.18(16) |
| Ru(1)−O(5) | 1.957(4) | O(3)−Ru(1)−O(4) | 93.28(19) |
| Ru(1)−O(6) | 1.986(4) | O(3)−Ru(1)−O(5) | 88.84(16) |
| Ru(2)−O(7) | 1.969(4) | O(3)−Ru(1)−O(6) | 178.96(16) |
| Ru(2)−O(8) | 1.962(4) | O(4)−Ru(1)−O(5) | 89.15(17) |
| Ru(2)−O(9) | 1.999(4) | O(5)−Ru(1)−O(6) | 90.24(16) |
| Ru(2)−O(10) | 2.019(4) | O(7)−Ru(2)−O(8) | 91.31(16) |
| Ru(2)−O(11) | 2.016(4) | O(7)−Ru(2)−O(9) | 87.84(17) |
| Ru(2)−O(12) | 1.997(4) | O(7)−Ru(2)−O(10) | 178.95(17) |
| O(5)−C(13) | 1.286(6) | O(7)−Ru(2)−O(11) | 88.02(16) |
| O(6)−C(11) | 1.292(6) | O(7)−Ru(2)−O(12) | 89.35(17) |
| O(7)−C(18) | 1.301(6) | O(8)−Ru(2)−O(9) | 91.35(17) |
| O(8)−C(16) | 1.305(6) | O(8)−Ru(2)−O(10) | 89.74(16) |
| C(11)−C(12) | 1.417(8) | O(8)−Ru(2)−O(11) | 178.62(17) |
| C(12)−C(13) | 1.436(8) | O(8)−Ru(2)−O(12) | 87.28(18) |
| C(13)−C(14) | 1.426(8) | | |
| C(14)−C(15) | 1.334(8) | | |
| C(15)−C(16) | 1.427(8) | | |
| C(16)−C(17) | 1.421(8) | | |
| C(17)−C(18) | 1.411(8) | | |
| C(18)−C(19) | 1.456(8) | | |
| C(11)−C(24) | 1.468(8) | | |
| C(12)−C(17) | 1.476(7) | | |
| C(19)−C(24) | 1.390(8) | | |
| Ru(1)−Ru(2) | 8.158 | | |

set in Tables 1 and 2. Each ruthenium ion is bonded to the bridge via two oxygen donor centers in a $\beta$-diketonate chelate fashion. The ruthenium centers lie virtually in the same plane as the bridging ligand, formulated as $QL^{2-}$. Each $RuO_6$ configuration is in a slightly distorted octahedral arrangement. The C−O and intraring distances (Table 2) collectively signify a delocalized state of the keto−enol form of metallated $QL^{2-}$ in **2**.[12] The average Ru<sup>III</sup>−O(acac⁻) distance of 2.009 Å agrees well with that in analogous reported complexes.[2a,3a,8c,9c,10,12] The average Ru<sup>III</sup>−O(QL²⁻) distance of 1.968 Å is slightly shorter (0.04 Å) than the average Ru<sup>III</sup>−O(acac⁻) bond length, indicating stronger binding to the bridge. The Ru−Ru distance in this first structurally characterized diruthenium complex of $QL^{2-}$ is 8.158 Å. The crystal structure of the diiron complex [{Fe(salen)}₂(QL²⁻)] has been reported.[6i]

The packing diagram along the *b* axis (Figure S2 in the Supporting Information) shows that two toluene molecules are packed between two molecules of **2**. The toluene at one end is linked with **2** via nonclassical short contacts (2.880 Å) between one of the carbon atoms of toluene and one of the hydrogen atoms associated with the methyl group of acac⁻. Similarly, the second toluene group is linked to the

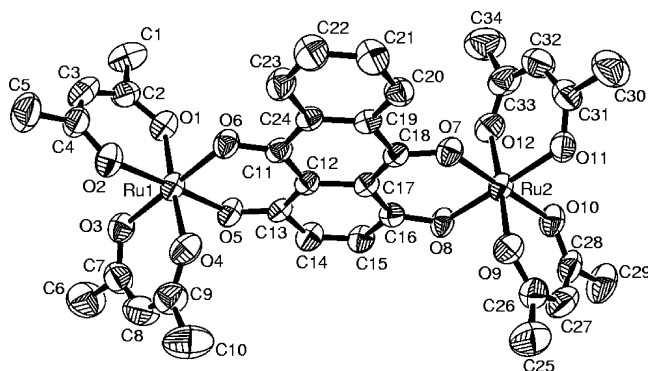second molecule of **2**, and the two in-between toluene rings are in contact with one another by 2.374 Å between the hydrogen atoms attached to the ring carbon centers (Figure S2 in the Supporting Information).

The ¹H NMR spectra of paramagnetic **1** and **2** exhibit signals from 17 to −29 ppm in CDCl₃ due to paramagnetic contact shifts (Figure 2, Table 3).[10a,13a,14] The diastereomeric **1** and **2** show clear differences in their chemical shifts (Table 3).

**Magnetic Properties of 2.** The variable temperature magnetic susceptibility of **2** in magnetic fields of 10 000 and 500 G show a broad maximum at 151 K and a steep increase



**Figure 1.** ORTEP diagram of **2**. Ellipsoids are drawn at 50% probability level.

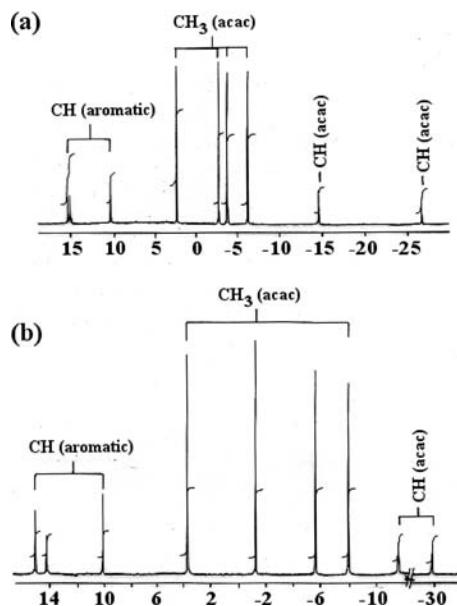(12) Chao, G. K. J.; Sime, R. L.; Sime, R. J. *Acta Crystallogr.* **1973**, *B29*, 2845.

**Figure 2.** $^1$H NMR spectra of (a) **1** and (b) **2** in CDCl$_3$.

**Table 3.** $^1$H NMR Spectral Data of **1** and **2** in CDCl$_3$

| | | $\delta$ (ppm) | |
|---|---|---|---|
| compound | aromatic protons | CH (acac) | CH$_3$ (acac) |
| **1** | 15.29 (1H) | −14.60 (1H) | 2.34 (3H), −2.80 (3H) |
| | 15.07 (1H) | −26.69 (1H) | −3.83 (3H), −6.28 (3H) |
| | 10.33 (1H) | | |
| **2** | 15.04 (1H) | −11.60 (1H) | 3.71 (3H), −1.26 (3H) |
| | 14.21 (1H) | −28.83 (1H) | −5.65 (3H), −7.99 (3H) |
| | 10.11 (1H) | | |

from 45 to 2 K (Figure 3). The susceptibility values for **2** are sensitive to the applied magnetic field at high temperatures but converge at very low temperatures. As a consequence, the magnetic moment varies from 2.23 to 0.50 and from 3.61 to 0.55 $\mu_B$ with the decrease in temperature at 10 000 and 500 G, respectively. The shape of the susceptibil-

(13) (a) Koiwa, T.; Masuda, Y.; Shono, J.; Kawamoto, Y.; Hoshino, Y.; Hashimoto, T.; Natarajan, K.; Shimizu, K. *Inorg. Chem.* **2004**, *43*, 6215. (b) Melendez, E.; Lopez, V.; Concolino, T.; Rheingold, A. L. *J. Organomet. Chem.* **2004**, *689*, 3082. (c) Frey, G. D.; Bell, Z. R.; Jeffery, J. C.; Ward, M. D. *Polyhedron* **2001**, *20*, 3231. (d) Chellamma, S.; Lieberman, M. *Inorg. Chem.* **2001**, *40*, 3177. (e) Melendez, E.; Guzei, I.; Rheingold, A. L. *J. Chem. Crystallogr.* **1999**, *29*, 399. (f) Hashimoto, T.; Endo, A.; Nagao, N.; Sato, G. P.; Natarajan, K.; Shimizu, K. *Inorg. Chem.* **1998**, *37*, 5211. (g) Reynolds, P. A.; Cable, J. W.; Sobolev, A. N.; Figgis, B. N. *J. Chem. Soc., Dalton Trans.* **1998**, 559. (h) Mashima, K.; Fukumoto, H.; Tani, K.; Haga, M.; NakamuraA., *Organometallics* **1998**, *17*, 410. (i) Bennett, M. A.; Neumann, H.; Willis, A. C.; Ballantini, V.; Pertici, P.; Mann, B. E. *Organometallics* **1997**, *16*, 2868. (j) Melendez, E.; Ilarraza, R.; Yap, G. P. A.; Rheingold, A. L. *J. Organomet. Chem.* **1996**, *522*, 1. (k) Knowles, T. S.; Howells, M. E.; Howlin, B. J.; Smith, G. W.; Amodio, C. A. *Polyhedron* **1994**, *13*, 2197. (l) Schneider, R.; Weyhermueller, T.; Wieghardt, K.; Nuber, B. *Inorg. Chem.* **1993**, *32*, 4925. (m) Schneider, R.; Wieghardt, K.; Nuber, B. *Inorg. Chem.* **1993**, *32*, 4935. (n) Matsuzawa, H.; Ohashi, Y.; Kaizu, Y.; Kobayashi, H. *Inorg. Chem.* **1988**, *27*, 2981. (o) Aynetchi, S.; Hitchcock, P. B.; Seddon, E. A.; Seddon, K. R.; Yousif, Y. Z.; Zora, J. A.; Stuckey, K. *Inorg. Chim. Acta* **1986**, *113*, L7–L9.
(14) (a) Eaton, D. R. *J. Am. Chem. Soc.* **1965**, *87*, 3097. (b) Palmer, R. A.; Fay, R. C.; Piper, T. S. *Inorg. Chem.* **1964**, *3*, 875. (c) Holm, R. H.; Cotton, F. A. *J. Am. Chem. Soc.* **1958**, *80*, 5658. (d) Fay, R. C.; Piper, T. S. *J. Am. Chem. Soc.* **1963**, *85*, 500. (e) Chen, J.-L.; Zhang, X.-U.; Zhang, L.-Y.; Shi, L.-X.; Chen, Z.-N. *Inorg. Chem.* **2005**, *44*, 1037.
(15) Kahn, O. *Molecular Magnetism*; VCH Publishers: New York, 1993; p 107.

**Table 4.** Magnetic Data for **2**

| | $H$ = 10 000 G | | $H$ = 500 G | |
|---|---|---|---|---|
| $g$ | 1.7 | 2 (fixed) | 1.8 | 2 (fixed) |
| $J$ (cm$^{-1}$) | −87.6 | −89.4 | −76.9 | −78.6 |
| TIP (emu mol$^{-1}$) | $6.0 \times 10^{-4}$ | $1.0 \times 10^{-4}$ | $4.1 \times 10^{-3}$ | $3.7 \times 10^{-3}$ |
| P (%) | 3.3 | 4.4 | 3.3 | 4.2 |
| $\sigma^{2a}$ | $6.5 \times 10^{-5}$ | $4.2 \times 10^{-4}$ | $9.2 \times 10^{-5}$ | $1.2 \times 10^{-4}$ |

$^a$ $\sigma^2 = \Sigma(\mu_{\text{eff.calc.}} - \mu_{\text{eff.exp.}})^2/\Sigma\mu_{\text{eff.exp.}}^2$

ity and moment curves are typical for complexes with antiferromagnetically coupled centers. The sharp increase of the susceptibility at very low temperatures is ascribed to small amounts of a paramagnetic impurity.

The field dependence of the magnetization measured at 2 and 300 K (Figures S3 and S4) is almost linear. At 2 K no evidence for the occurrence of ferromagnetic coupling is observed. However, at 300 K and at very low fields the magnetization is slightly higher to the corresponding Brillouin function's curve.

The magnetic behavior of **2** has been fitted using the eq (1) based on the van Vleck approximation of the antiferromagnetic coupling[15] with a model that considers the exchange spin Hamiltonian $H = -2 J S_1 S_2$ ($S_1 = S_2 = 1/2$) operating over two antiferromagnetically coupled S = 1/2 Ru$^{III}$ centers,[15] together with a temperature independent paramagnetism (TIP) term and the presence of an (S = 1) paramagnetic impurity (equation 1).

$$\chi' = (1-P)\,\chi + P\,\frac{2\,Ng^2\beta^2}{3kT} \qquad (1)$$

where:

$$\chi = \frac{Ng^2\beta^2}{kT}\frac{2\,\exp\,(2J/kT)}{1+3\,\exp\,(2J/kT)} + TIP$$

The fit at 10 000 and 500 G, gives good agreement between the experimental and calculated curves (Figure 3). The parameters obtained in the best fits and the accordance factors are collected in Table 4. The fit of the experimental data by fixing g = 2 (Table 4) gives very similar magnetic parameters with a poorer accordance factor. The obtained $J$ values −87.6/−89.4 cm$^{-1}$ for **2** are close to those reported[8a,13l] for [(acac)$_2$Ru$^{III}$($\mu$-boptz)Ru$^{III}$(acac)$_2$] (boptz =
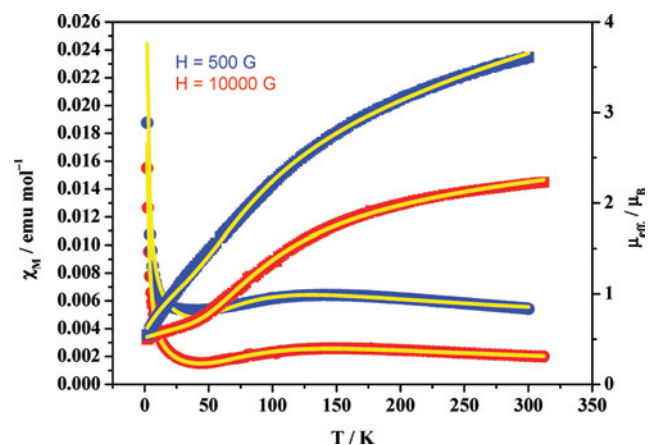


**Figure 3.** Temperature dependence of the molar susceptibility (circles) and magnetic moment (squares) for **2** in magnetic fields of 10 000 (red) and 500 (blue) G. Solid lines result from least-squares fits using the model described in the text.
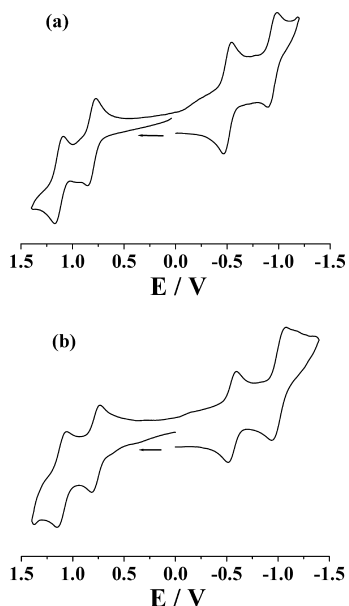
**Figure 4.** Cyclic voltammograms of (a) **1** and (b) **2** in CH$_3$CN/0.1 M Et$_4$NClO$_4$ versus SCE at 298 K (scan rate 50 mV s$^{-1}$).

**Table 5.** Redox Potentials$^{a,b}$ and Comproportionation Constant Values ($K_c$)$^c$ for **1** and **2**

| compound | $E°_{298}$ [V] ($\Delta E$ [mV]) | | | | $K_c$ |
|---|---|---|---|---|---|
| **1** | 1.13 | 0.82 | −0.51 | −0.94 | $K_{c1} = 10^{5.2}$ |
| | (78) | (79) | (79) | (84) | $K_{c2} = 10^{7.3}$ |
| **2** | 1.11 | 0.77 | −0.55 | −1.01 | $K_{c1} = 10^{5.7}$ |
| | (86) | (73) | (84) | (127) | $K_{c2} = 10^{7.8}$ |

$^a$ Potentials $E°_{298}$/V ($\Delta E$/mV) versus SCE. $^b$ In CH$_3$CN/0.1 M Et$_4$NClO$_4$/ scan rate 50 mV s$^{-1}$ $^c$ $RT$ ln$K_c = nF(\Delta E)$.

3,6-bis(2-oxidophenyl)-1,2,4,5-tetrazine) and [L(acac)Ru$^{III}$($\mu$-O)Ru$^{III}$(acac)L](PF$_6$)$_2$ (L = 1,7-trimethyl-1,4,7-triazacy-clononane) at −36.7 and −53 cm$^{-1}$, respectively, but are less pronounced than the −300 to −700 cm$^{-1}$ observed in several ($\mu$-alkoxo)bis($\mu$-carboxylato)diruthenium(III) complexes.[16]

**Electrochemistry, UV-vis-NIR Spectroelectrochemistry and EPR Investigations.** Diastereomers such as **1** and **2** are likely to exhibit similar redox processes, and the potentials are thus expected to be very close.[8c,10d,11] Both **1** and **2** display two successive one-electron oxidation and reduction processes (Figure 4, Table 5) with the potentials for the rac isomer **1** slightly higher than those of the meso analogue **2**. The potential differences between successive oxidation processes lead to comproportionation constants $K_{c1}$ ($RT$ ln$K_c$ = $nF(\Delta E)^{17}$) of $10^{5.2}$ and $10^{5.7}$ for $1^+$ and $2^+$, respectively, the $K_{c2}$ values for the reduction to $1^-$ and $2^-$ are $10^{7.3}$ and $10^{7.8}$, respectively. The corresponding complexes [{Ru$^{II}$ (bpy)$_2$}$_2$($\mu$-QL$^{2-}$)]$^{2+}$ [6b] and [{Ru$^{II}$(pap)$_2$}$_2$($\mu$-QL$^{2-}$)]$^{2+}$ [6a] exhibited $K_{c1}$ values of 3.7 × 10$^4$ and 8.2 × 10$^4$, respectively, for the oxidation. The oxidation processes in the bpy complex were assigned as Ru$^{II}$/Ru$^{III}$-based couples,[6b] whereas the

exchange of bpy by pap was reported to involve a ligand-based first oxidation to {(pap)$_2$Ru$^{II}$($\mu$-QL$^{•-}$)Ru$^{II}$(pap)$_2$}$^{3+}$, followed by metal oxidation to {(pap)$_2$Ru$^{II}$($\mu$-QL$^{•-}$)Ru$^{II}$₁(pap)$_2$}$^{4+}$ or {(pap)$_2$Ru$^{III}$($\mu$-QL$^{•-}$)Ru$^{III}$(pap)$_2$}$^{4+}$.[6a]

In **1** and **2**, both the metal ion pair and the bridging ligand (QL$^{n-}$) (Scheme 2) are capable of undergoing four reversible one-electron transfers at reasonable potentials.

The combinations arising from this special situation are summarized in Scheme 3 (L = quinizarine).

Therefore, the redox processes of the diastereomeric [(acac)$_2$Ru($\mu$-QL)Ru(acac)$_2$]$^n$ (**1** and **2**) (Figure 4) have been investigated via spectroelectrochemistry and EPR for the accessible states with $n$ = +2, +1, 0, −1, and −2 to establish the likely sites of electron transfer.

The UV-vis-NIR spectroelectrochemical features in the $n$ = +2, +1, 0, −1, and −2 redox states are similar for **1** and **2**, except for slight variations in the band positions and intensities (Figure S5 in the Supporting Information, Figure 5, and Table 6). The intense ligand-to-metal charge-transfer (LMCT, electron-rich QL$^{2-}$/acac$^-$ to Ru$^{III}$) band near 550 nm in **1** or **2** is diminished to almost half of its intensity on moving to $1^+$ or $2^+$ with the concomitant growth of a new band near 600 nm of similar intensity. Moreover, the one-electron oxidized species exhibit a low-energy intense band near 1390 nm ($\varepsilon \approx 8000$ M$^{-1}$ cm$^{-1}$) with bandwidths $\Delta \nu_{1/2}$ of about 2500 cm$^{-1}$ for $1^+$ and $2^+$. This low-energy band is replaced on second oxidation to $1^{2+}$ or $2^{2+}$ by a stronger absorption at about 1100 nm. Most revealingly, the intermediates $1^+$ and $2^+$ failed to show an EPR signal even at 4 K, probably due to rapid relaxation. The spectral signatures for $1^+$ and $2^+$ are therefore considered to reflect a metal-based first-oxidation process, leading to the formation of a mixed-valent {Ru$^{III}$(QL$^{2-}$)Ru$^{IV}$} formulation to best describe this intermediate (Scheme 3).

Though d$^4$d$^5$ configured mixed-valent species with distinct IVCT (intervalence charge transfer) bands are less common,[8a,10a,18] IVCT absorptions ascribed to Ru$^{III}$−Ru$^{IV}$ intermediates have been reported recently, for example for {($\mu$-gbha)[Ru(acac)$_2$]$_2$}$^+$ (gbha$^{2-}$ = 1,4-bis(2-phenolato)-1,4-diazabutadiene)[8b] or in a C$_4$-linked bis[tris($\beta$-diketonato)ruthenium] complex.[18b] Assuming a Ru$^{III}$−Ru$^{IV}$ formulation, the near-infrared bands at around 1390 nm (Table 6) are assigned to IVCT transitions for $1^+$ and $2^+$. The calculated bandwidths of about 4070 cm$^{-1}$ [$\nu_{IVCT}$: 1395 nm (7168 cm$^{-1}$) and 1390 nm (7194 cm$^{-1}$) for $1^+$ and $2^+$, respectively], according to the Hush formula of localized class II mixed valent systems, [$\Delta \nu_{1/2}$ (calcd) = (2310$\nu_{IVCT}$)$^{1/2}$],[19] are much higher than those determined experimentally at 2420 and 2650 cm$^{-1}$ for $1^+$ and $2^+$, respectively. The narrower IVCT bands in combination with the $K_c$ values support either a valence-averaged class III or a borderline class II−III hybrid situation. Borderline class II−III situations have been

(16) (a) Mikata, Y.; Takeshita, N.; Miyazu, T.; Miyata, Y.; Tanase, T.; Kinoshita, I.; Ichimura, A.; Mori, W.; Takamizawa, S.; Yano, S. *J. Chem. Soc., Dalton Trans.* **1998**, 1969. (b) Obata, M.; Tanihara, N.; Nakai, M.; Harada, M.; Aimoto, S.; Yamazaki, I.; Ichimura, A.; Kinoshita, I.; Mikuriya, M.; Hoshino, M.; Yano, S. *Dalton Trans.* **2004**, 3283.
(17) Robin, M. B.; Day, P. *Adv. Inorg. Chem. Radiochem.* **1967**, *10*, 247.

(18) (a) Demadis, K. D.; Hartshorn, C. M.; Meyer, T. J. *Chem. Rev.* **2001**, *101*, 2655. (b) Hoshino, Y.; Higuchi, S.; Fiedler, J.; Su, C.-Y.; Knödler, A.; Schwederski, B.; Sarkar, B.; Hartmann, H.; Kaim, W. *Angew. Chem., Int. Ed.* **2003**, *42*, 674. (c) Naklicki, M. L.; White, C. A.; Kondratiev, V. V.; Crutchley, R. J. *Inorg. Chim. Acta* **1996**, *242*, 63.
(19) Hush, N. S. *Prog. Inorg. Chem.* **1967**, *8*, 391.
(20) Creutz, C. *Prog. Inorg. Chem.* **1983**, *30*, 1.

**Scheme 2**

$$\text{Ru}^{II}\text{Ru}^{II} \underset{+e}{\overset{-e}{\rightleftarrows}} \text{Ru}^{II}\text{Ru}^{III} \underset{+e}{\overset{-e}{\rightleftarrows}} \text{Ru}^{III}\text{Ru}^{III} \underset{+e}{\overset{-e}{\rightleftarrows}} \text{Ru}^{III}\text{Ru}^{IV} \underset{+e}{\overset{-e}{\rightleftarrows}} \text{Ru}^{IV}\text{Ru}^{IV}$$

$$[\text{anthracene-}O^-,O^-]^{4-} \underset{+e^-}{\overset{-e^-}{\rightleftarrows}} [\text{anthracene-}O^-,O^\bullet]^{3-} \underset{+e^-}{\overset{-e^-}{\rightleftarrows}} [\text{anthraquinone-}O,O^-]^{2-} \underse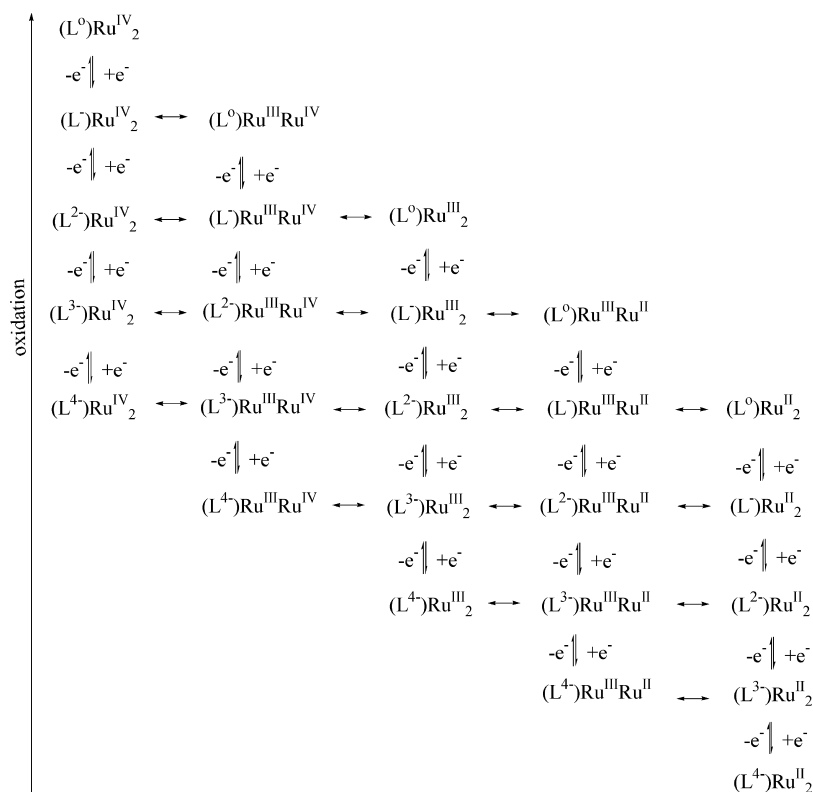t{+e^-}{\overset{-e^-}{\rightleftarrows}} [\text{anthraquinone-}O,O^\bullet]^{-} \underset{+e^-}{\overset{-e^-}{\rightleftarrows}} \text{anthraquinone-}O,O$$

$$\mathbf{QL^{2-}}$$

**Scheme 3**

oxidation ↑

$$(\text{L}^{o})\text{Ru}^{IV}_2$$
$$-e^- \| +e^-$$
$$(\text{L}^{-})\text{Ru}^{IV}_2 \leftrightarrow (\text{L}^{o})\text{Ru}^{III}\text{Ru}^{IV}$$
$$-e^- \| +e^- \qquad -e^- \| +e^-$$
$$(\text{L}^{2-})\text{Ru}^{IV}_2 \leftrightarrow (\text{L}^{-})\text{Ru}^{III}\text{Ru}^{IV} \leftrightarrow (\text{L}^{o})\text{Ru}^{III}_2$$
$$-e^- \| +e^- \qquad -e^- \| +e^- \qquad -e^- \| +e^-$$
$$(\text{L}^{3-})\text{Ru}^{IV}_2 \leftrightarrow (\text{L}^{2-})\text{Ru}^{III}\text{Ru}^{IV} \leftrightarrow (\text{L}^{-})\text{Ru}^{III}_2 \leftrightarrow (\text{L}^{o})\text{Ru}^{III}\text{Ru}^{II}$$
$$-e^- \| +e^- \qquad -e^- \| +e^- \qquad -e^- \| +e^- \qquad -e^- \| +e^-$$
$$(\text{L}^{4-})\text{Ru}^{IV}_2 \leftrightarrow (\text{L}^{3-})\text{Ru}^{III}\text{Ru}^{IV} \leftrightarrow (\text{L}^{2-})\text{Ru}^{III}_2 \leftrightarrow (\text{L}^{-})\text{Ru}^{III}\text{Ru}^{II} \leftrightarrow (\text{L}^{o})\text{Ru}^{II}_2$$
$$-e^- \| +e^- \qquad -e^- \| +e^- \qquad -e^- \| +e^- \qquad -e^- \| +e^-$$
$$(\text{L}^{4-})\text{Ru}^{III}\text{Ru}^{IV} \leftrightarrow (\text{L}^{3-})\text{Ru}^{III}_2 \leftrightarrow (\text{L}^{2-})\text{Ru}^{III}\text{Ru}^{II} \leftrightarrow (\text{L}^{-})\text{Ru}^{II}_2$$
$$-e^- \| +e^- \qquad -e^- \| +e^- \qquad -e^- \| +e^-$$
$$(\text{L}^{4-})\text{Ru}^{III}_2 \leftrightarrow (\text{L}^{3-})\text{Ru}^{III}\text{Ru}^{II} \leftrightarrow (\text{L}^{2-})\text{Ru}^{II}_2$$
$$-e^- \| +e^- \qquad -e^- \| +e^-$$
$$(\text{L}^{4-})\text{Ru}^{III}\text{Ru}^{II} \leftrightarrow (\text{L}^{3-})\text{Ru}^{II}_2$$
$$-e^- \| +e^-$$
$$(\text{L}^{4-})\text{Ru}^{II}_2$$

**Table 6.** UV-Vis-NIR Data for **1** and **2** in Various Oxidation States From OTTLE Spectroelectrochemistry in $CH_2Cl_2$

| compound | $\lambda$[nm] ($\varepsilon$ [$M^{-1}cm^{-1}$]) |
|---|---|
| $\mathbf{1^{2+}}$ | 1101(10 900), 677(8200), 515(9600), 390sh, 280sh, 249(38 000), 230(38 900) |
| $\mathbf{1^+}$ | 1395(8200), 611(10 200), 509(10 900), 338(13 300), 285sh, 251(37 700), 220(36 500) |
| $\mathbf{1}$ | 548(19 900), 345(13 100), 276sh, 252(43 200), 217(36 400) |
| $\mathbf{1^-}$ | 886(23 100), 507(10 100), 433sh, 385(12 700), 270(40 000), 254(40 500), 216(35 600) |
| $\mathbf{1^{2-}}$ | 1140sh, 868(38 300), 488(14 300), 430sh, 365(10 400), 271(42 900), 253(46 400), 215(36 100) |
| $\mathbf{2^{2+}}$ | 1095(11 300), 670(8900), 516(9700), 385sh, 283sh, 245(44 800), 220(45 700) |
| $\mathbf{2^+}$ | 1390(8400), 611(10 700), 505(11 000), 343sh, 285sh, 251(42 800), 219(41 700) |
| $\mathbf{2}$ | 549(19 800), 346(15 100), 272sh, 252(46 000), 217(39 200) |
| $\mathbf{2^-}$ | 885(18 600), 512(11 200), 427sh, 376(13 700), 270(43 900), 255(45 100), 217(39 200) |
| $\mathbf{2^{2-}}$ | 1155sh, 868(30 500), 488(11 900), 426sh, 363(8400), 272(37 200), 253(39 300), 215(29 000) |

established in $d^5d^6$ ($Ru^{III}-Ru^{II}$) mixed-valent systems, for example for the pyrazine-bridged Creutz–Taube ion[20] or tppz-bridged diruthenium complexes (tppz = 2,3,5,6-tetrakis(2-pyridyl)pyrazine).[21] The absence of an EPR signal even at 4 K signifies rapid relaxation, which is not untypical for less strongly coupled mixed-valent intermediates[22a] and which is not unexpected for a $d^4d^5$ combination.[8b,22b]

Upon further one-electron oxidation to $\mathbf{1^{2+}}$ or $\mathbf{2^{2+}}$, the IVCT band intensity vanishes completely with the concomitant growth of an absorption near 1100 nm, which can be assigned to an LMCT transition from electron-rich $QL^{2-}/acac^-$ to the oxidized metals in [(acac)$_2$Ru$^{IV}$($\mu$-QL$^{2-}$)Ru$^{IV}$(acac)$_2$]$^{2+}$. The alternative {(acac)$_2$Ru$^{III}$($\mu$-QL$^{o}$)Ru$^{III}$(acac)$_2$}$^{2+}$ with a fully oxidized quinone bridge for the doubly oxidized species is ruled out primarily because of the intense low-energy LMCT transition.

The substantial reduction of the LMCT band intensity on one-electron reduction to $\mathbf{1^-}$ or $\mathbf{2^-}$, the simultaneous growth of an intense absorption near 880 nm, the absence of a band in the near-IR region (Figure S5 in the Supporting Information and Figure 5), and the metal-based spin as evident from the EPR signals at 4 or 110 K ($g_1 = 2.25$, $g_2 = 2.25$, $g_3 = $
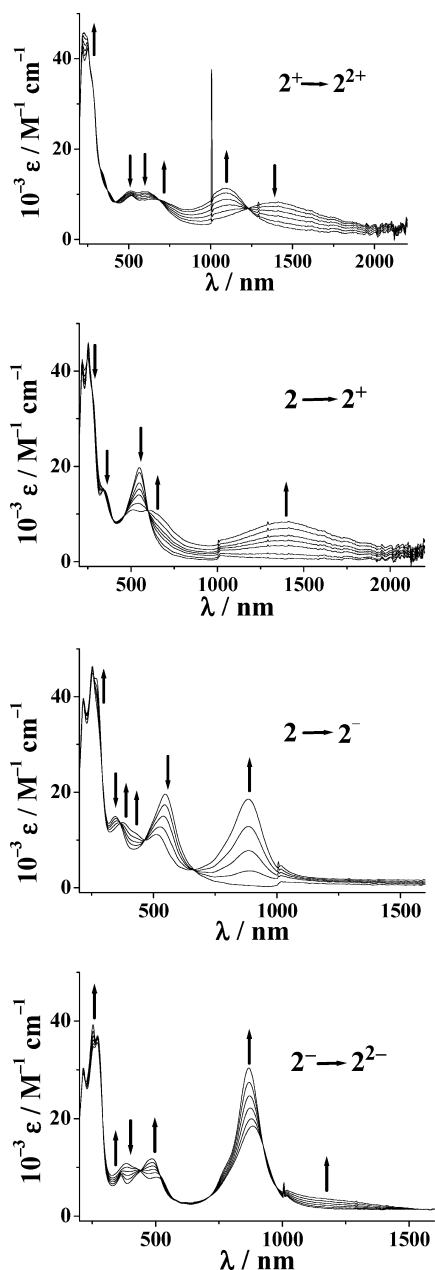
**Figure 5.** OTTLE spectroelectrochemistry for $2^n$ in $CH_3CN/0.1$ M $Bu_4NPF_6$.

LMCT transition between electron rich $QL^{4-}$ and ruthenium(III) in $[(acac)_2Ru^{III}(\mu\text{-}QL^{4-})Ru^{III}(acac)_2]^{2-}$. Yet, the alternative formulation $\{(acac)_2Ru^{II}(\mu\text{-}QL^{2-})Ru^{II}(acac)_2\}^{2-}$ with $Ru^{II} \rightarrow QL^{2-}$ MLCT character of the low-energy transition is also conceivable, reflecting the pronounced tendency of ruthenium−quinone systems for orbital mixing and thus delocalized bonding;[1,2e] the assignments given here are thus tentative on the basis of the most plausible interpretations of absorption and magnetic resonance data.

## Conclusion

The extended (i.e., four-step) redox series potential of *both* the bridging ligand and the metal pair as outlined in Scheme 2 causes an increased number of accessible charge states and a large variety of reasonable alternative combinations in the complex (Scheme 3). Notwithstanding the redox ambiguity, we maintain that the magnetic exchange in the neutral compounds and the mixed-valence coupling occur via a hole-transfer superexchange involving the carbonyl-centered $\pi$ HOMO of the ligand dianion and that the reduction of the complexes is largely ligand-centered, whereas the oxidation is more metal-based.

## Experimental Section

The starting complex $Ru(acac)_2(CH_3CN)_2$,[24] was prepared according to the reported procedure. 1,4-Dihydroxy-9,10-anthraquinone (quinizarine, $QLH_2$) was obtained from Aldrich. Other chemicals and solvents were reagent grade and used as received. For spectroscopic and electrochemical studies, HPLC-grade solvents were used.

UV-vis-NIR spectroelectrochemical studies were performed in $CH_3CN/0.1$ M $Bu_4NPF_6$ at 298 K using an optically transparent thin layer electrode (OTTLE) cell[25] mounted in the sample compartment of a J&M TIDAS spectrophotometer. FTIR spectra were taken on a Nicolet spectrophotometer with samples prepared as KBr pellets. Solution electrical conductivity was checked using a Systronic 305 conductivity bridge. $^1H$ NMR spectra were obtained with a 300 MHz Varian FT spectrometer. The EPR measurements were made in a two-electrode capillary tube[26] with

1.94 and $g_1 = 2.21$, $g_2 = 2.21$, $g_3 = 1.87$ for $1^-$ and $2^-$, respectively, Figure S6 in the Supporting Information) collectively suggest a quinone-based first reduction, leading to the formation of $[(acac)_2Ru^{III}(\mu\text{-}QL^{3\bullet-})Ru^{III}(acac)_2]^-$. The alternative with the metal as the center of the reduction, leading to $[(acac)_2Ru^{III}(\mu\text{-}QL^{2-})Ru^{II}(acac)_2]^-$ or the redox redistributed form $[(acac)_2Ru^{II}(\mu\text{-}QL^{\bullet-})Ru^{II}(acac)_2]^-$ are less compatible with metal-based spin and absent near-IR absorption. The formulation $[(acac)_2Ru^{III}(\mu\text{-}QL^{3\bullet-})Ru^{III}(acac)_2]^-$ involves a three-spin situation[23] with ↑↓↑ arrangement, where antiferromagnetic coupling causes one peripheral (here, metal-centered) spin to remain.

Upon further one-electron reduction to $1^{2-}$ or $2^{2-}$, the long-wavelength LMCT band gets more intense and slightly blue-shifted to 868 nm, it is attributed to the

(21) (a) Ghumaan, S.; Sarkar, B.; Chanda, N.; Sieger, M.; Fiedler, J.; Kaim, W.; Lahiri, G. K. *Inorg. Chem.* **2006**, *45*, 7955. (b) Chanda, N.; Sarkar, B.; Fiedler, J.; Kaim, W.; Lahiri, G. K. *Dalton Trans.* **2003**, 3550. (c) Chanda, N.; Sarkar, B.; Kar, S.; Fiedler, J.; Kaim, W.; Lahiri, G. K. *Inorg. Chem.* **2004**, *43*, 5128. (d) Chanda, N.; Laye, R. H.; Chakraborty, S.; Paul, R. L.; Jeffery, J. C.; Ward, M. D.; Lahiri, G. K. *J. Chem. Soc., Dalton Trans.* **2002**, 3496. (e) Koley, M.; Sarkar, B.; Ghumaan, S.; Bulak, E.; Fiedler, J.; Kaim, W.; Lahiri, G. K. *Inorg. Chem.* **2007**, *46*, 3736. (f) Hartshorn, V.; Daire, N.; Tondreau, V.; Loeb, B.; Meyer, T. J.; White, P. S. *Inorg. Chem.* **1999**, *38*, 3200.
(22) (a) Scheiring, T.; Kaim, W.; Olabe, J. A.; Parise, R. A.; Fiedler, J. *Inorg. Chim. Acta* **2000**, *300−302*, 125. (b) Kaim, W.; Lahiri, G. K. *Angew. Chem.* **2007**, *119*, 1808;. *Angew. Chem. Int. Ed.* **2007**, *46*, 1778.
(23) Ye, S.; Sarkar, B.; Lissner, F.; Schleid, Th.; van Slageren, J.; Fiedler, J.; Kaim, W. *Angew. Chem.* **2005**, *117*, 2140;. *Angew. Chem. Int. Ed.* **2005**, *44*, 2103.
(24) Kobayashi, T.; Nishina, Y.; Shimizu, K. G.; Satô, G. P. *Chem. Lett.* **1988**, 1137.
(25) Krejcik, M.; Danek, M.; Hartl, F. *J. Electroanal. Chem.* **1991**, *317*, 179.
(26) Kaim, W.; Ernst, S.; Kasack, V. *J. Am. Chem. Soc.* **1990**, *112*, 173.

an X-band (9.5 GHz) Bruker system ESP300, equipped with a Bruker ER035 M gaussmeter and a HP 5350B microwave counter. Cyclic voltammetric, differential pulse voltammetric, and coulometric measurements were carried out using a PAR model 273A electrochemistry system. Platinum wire working and auxiliary electrodes and an aqueous saturated calomel reference electrode (SCE) were used in a three-electrode configuration. The supporting electrolyte was 0.1 M $Et_4NClO_4$, and the solute concentration was ca. $10^{-3}$ M. The half-wave potential $E^o{}_{298}$ was set equal to $0.5(E_{pa} + E_{pc})$, where $E_{pa}$ and $E_{pc}$ are anodic and cathodic cyclic voltammetric peak potentials, respectively. A platinum wire-gauze working electrode was used in coulometric experiments. The elemental analysis was carried out with a PerkinElmer 240C elemental analyzer. Electrospray mass spectra were recorded on a Micromass Q-ToF mass spectrometer.

**Synthesis of** *rac*-[{(acac)₂Ru^III}₂($\mu$-QL²⁻)] (1), *meso*-[{(acac)₂Ru^III}₂($\mu$-QL²⁻)] (2). The starting complex [Ru(acac)₂(CH₃CN)₂] (100 mg, 0.26 mmol), 1,4-dihydroxy-9,10-anthraquinone (QLH₂) ligand (32 mg, 0.13 mmol), and sodium acetate (25 mg, 0.3 mmol) were taken in 20 mL ethanol, and the mixture was heated at reflux for 4 h. The initial orange color of the solution gradually changed to violet. The solvent was then removed under reduced pressure. The solid residue thus obtained was purified using a silica gel (60−120 mesh) column. Initially, a red solution corresponding to Ru(acac)₃ was eluted by CH₂Cl₂/CH₃CN (50:1). With CH₂Cl₂/CH₃CN (30:1), a blue-violet solution corresponding to the mixture of **1** and **2** was eluted. The mixture of diastereomers **1** and **2** was then separated on a preparatory TLC plate (silica gel 60 F₂₅₄) using CH₂Cl₂/CH₃CN (50:1). **1**: Yield, 33 mg (30%). Anal. Calcd (Found): C, 48.69 (48.73); H, 4.09 (3.90). **2**: Yield, 30 mg (27%). Anal. Calcd (Found): C, 48.69 (48.98); H, 4.09 (4.19).

**Crystal Structure Determination of 2.** Single crystals were grown by slow evaporation of a 1:1 toluene−acetonitrile mixture of **2**. X-ray data of **2** were collected on a PC-controlled Enraf-Nonius CAD-4 (MACH-3) single crystal X-ray diffractometer using Mo Kα radiation. Significant crystallographic parameters are listed in Table 1. The structure was solved and refined by full-matrix least-squares techniques on $F^2$ using *SHELX-97* (*SHELXTL* program package).[27]

**Magnetic Measurements.** The variable-temperature magnetic susceptibilities were measured on polycrystalline samples with a Quantum Design MPMSXL SQUID (Superconducting Quantum Interference Device) susceptometer over a temperature range of 2 to 300 K. Each raw data field was corrected for the diamagnetic contributions to the susceptibility from both the sample holder and the complex. The molar diamagnetic corrections were calculated on the basis of Pascal constants. The fit of the experimental data was carried out using the *MATLAB V.5.1.0.421* program.

**Supporting Information Available:** X-ray crystallographic file in CIF format for **2**, mass spectra of **1** and **2** in CH₂Cl₂, packing diagram of **2**, field dependence of the magnetization for **2** at 2 and 300 K, OTTLE spectroelectrochemistry for **1**ⁿ, EPR spectrum of **2**⁻ in CH₃CN at 4 K. This material is available free of charge via the Internet at http://pubs.acs.org.

(27) Sheldrick, G. M. *SHELXS−97, Program for Crystal Structure Solution and Refinement*; University of Göttingen: Göttingen, Germany, 1997.